Electron impact dissociative ionization and the subsequent ion–molecule reactions in a methane beam

Cechan Tian [1], C.R. Vidal

Max Planck Institut für Extraterrestrische Physik, P.O. Box 1603, 85740 Garching, Germany

Abstract

The cross-sections of the electron impact dissociative ionization of methane have been measured for electron energies from threshold to 100 eV. For CH_4^+ the results agree with the existing measurements. For the fragments of CH_3^+, CH_2^+, CH^+, and C^+, our results overlap with the previous results within their reported error limits. These earlier measurements exceed their given error limits and hence are inconsistent. At higher backing pressures the subsequent ion–molecule reactions and their product ions have been measured. © 1997 Elsevier Science B.V.

1. Introduction

It has been realized for quite some time that ion–molecule reactions play a dominant role in interstellar clouds since the rate constants of ion–molecule reactions can be as high as 1×10^{-8} cm^3/s, compared to those of neutral–neutral reactions ranging around 10^{-11} cm^3/s [1,2]. In producing the reactant ions, the direct and dissociative ionization of molecules due to electron impact are very important since the cross-section of these processes is much higher than other collisional processes involving species in their ground states. In dense interstellar clouds, the density of electrons, which can be generated by cosmic ray particles and the radiation from the sun, can reach the order of 10^{-8} relative to the abundance of hydrogen [2]. It is the highest among all the charged particles. This is one of the reasons

why the cross-section of dissociative ionization of molecules due to electron impact has been considered for quite some time [3]. Clarifying measurements of the ionization cross-sections are still of great interest [4–6], and many groups are making different efforts to get more reliable data. However, the agreement between these different measurements has not been satisfactory. Especially for smaller fragments, the results exceed the claimed errors. In this paper we will report our results on the measurement of the cross-sections of dissociative ionization of methane for electron energies from threshold to 100 eV. Careful measurements and calibrations have been made. We will discuss the possible sources of errors in the different measurement techniques. At higher backing pressures, we also observed extensive ion–molecule reactions. The relative productions were measured for the electron energies from threshold to 100 eV. The results were explained based on the experimental cross-sections of dissociative ionization, and the rate-constant and the product ratio

---

[1] Alexander von Humboldt fellow.

measurement of ion—molecule reactions in the literature.

2. Experimental set-up

The experimental set-up is shown in Fig. 1(a). A methane beam is provided by expanding methane through a supersonic pulsed nozzle with a diameter of the orifice of 0.7 mm. The commercial methane has a purity of 99.9995%. The backing pressure at the gas valve is on the order of 0.3 bar. During the measurement the backing pressure is kept stable to ±0.2%. The electronic pulse applied to the pulsed nozzle has a duration of 160 μs. The gas jet passes through a skimmer, which has a diameter of 1.27 mm and is located about 3 cm below the pulsed nozzle. The resultant molecular beam is about 2 mm in diameter, the density of the methane molecules in the beam is estimated to be on the order of $10^{11-12}/cm^3$. The molecular beam is crossed by a pulsed electron beam at right angles. Without operation of the pulsed nozzle the vacuum of the system is on the order of 2×10^{-7} mbar. With operation of the pulsed nozzle at 20 Hz the background vacuum rises to about 6×10^{-6} mbar.

The molecular beam is ionized by a pulsed electron gun. The excitation and detection time sequence is shown in Fig. 1(b). The electron beam pulse has a duration of 200 ns. The repellor and extractor are biased for about 20 μs after the electron beam is turned off. In this pulsed extraction configuration the electron beam ionizes the molecular beam in a field free region. Therefore the electron beam is not deflected by the extraction field and the distribution of the electron energy is only determined by the configuration of the electron gun. The pulsed extraction field is about 40 V/cm, where the saturation of extraction was observed. The overall ion energy is about 10 eV. The ions are extracted into the ion optics, which focus the ions into a quadrupole mass spectrometer. The interaction region, the ion optics, and the entrance of the mass spectrometer are magnetically shielded to eliminate the earth magnetic field and any other interference outside. We have simulated the ion trajectories on a computer using the SIMION program. It shows that all the ions with an initial kinetic energy less than 3 eV can be
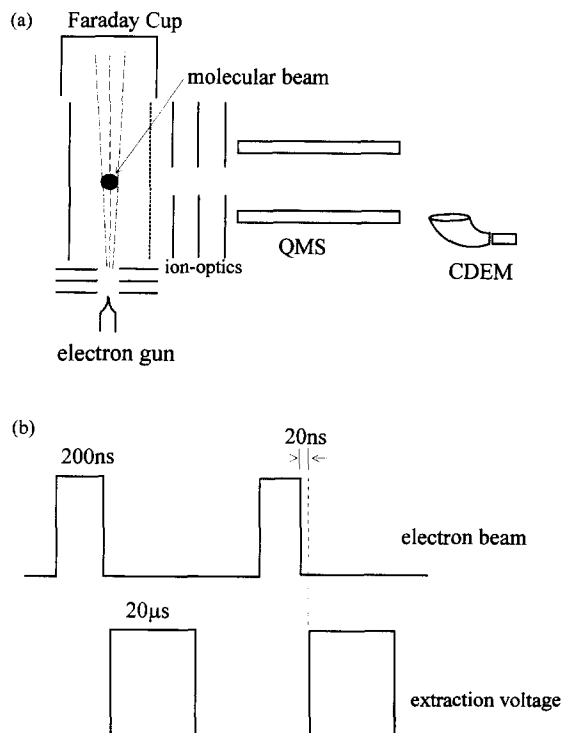

Fig. 1. (a) The experimental configuration, QMS-quadrupole mass spectrometer, CDEM-continuous dynode electromultiplier. (b) The time sequence of the electron pulse and the pulsed extraction field.

completely collected into the entrance of the mass spectrometer. The ions were accelerated further to about 2400 eV by the biased voltage of the detector and were detected by a continuous dynode electron multiplier (CDEM), which is located off-axis to eliminate the possibly optical noise along the axis of the quadrupole. The ion pulses are amplified to about 0.7 V with a fast preamplifier (SR445) and counted by a photoncounter (SR400). The discriminator of the photon counter was set to the maximum (0.3 V) to eliminate any electronic noises.

The pulsed electron beam is generated by a self-made electron gun, which can emit at least 30 μA at an electron energy of 20 eV. In the experiment the electron beam current was limited to 10 μA so that the maximum ion counts in each pulse is less than 20. The ions reach the detection region in a time duration of about 20 μs, so that there is little possibility for the ion signal to pile up. A pulsed high voltage with a width of about 200 ns was applied to

the first lens of the electron gun so that the output electron beam was pulsed with a duration of about 200 ns. The Faraday Cup signal showed that the rise and fall time of the electron beam was less than 20 ns. The electron energy of the electron gun was controlled through a computer interface and can be scanned in steps of 0.05 eV. The FWHM of the electron energy distribution of the electron beam was estimated to be 0.5 eV. The electron energy was calibrated to the appearance potential of CH_4^+ at 12.6 eV. The electron energy was scanned in steps of 2 eV. At every point the counts were accumulated over 200 gas pulses. For every fragment the dependence of counts on electron energy was measured at least five times. Finally an average was taken for the cross-section value calculations.

In measuring the cross-section for direct ionization, we mixed methane with Ne. The ionization cross-sections of CH_4, as a function of electron energy, are obtained by measuring the ion-yield of CH_4^+ relative to the well-established cross-section of Ne [7] according to the equation [8]

$$\sigma_{CH_4^+} = \frac{n_{Ne} I_{CH_4^+}}{n_{CH_4} I_{Ne^+}} \sigma_{Ne^+} S_{CH_4,Ne},$$ (1)

where σ is the cross-section of the relevant species, I is the ion signal count rate, n is the number density. $S_{CH_4,Ne}$ are the instrumental effects which may give rise to different detection efficiencies for CH_4^+ and Ne^+ and which include the relative production rate at the nozzle as well as the relative sensitivity of the quadrupole mass spectrometer. The relative number density of CH_4 and Ne was determined by measuring the partial pressure of the gases in a mixing bottle with a MKS Baratron manometer, neglecting the possible nonuniformity in the gas jet because of the similar mass of both gases [8]. At about every 5 eV both the count rates of CH_4^+ and Ne^+ were measured, the relative count rate was used to determine the cross-section for CH_4^+. In measuring the dissociative ionization cross-section of CH_3^+, CH_2^+, CH^+, and C^+, only pure methane was used. The measurements for the smaller fragments were normalized to the result of CH_4^+, so that the accuracy of the result of Ne does not affect the relative measurement of the smaller fragments. No attempt was made to measure the cross-section for the frag-

ments of H_2^+ and H^+, since in the dissociative ionization of methane, the kinetic energy of these fragments are much bigger [9,10], the collection efficiency will not be unity, and the transmission of the ions through the quadrupole will not be the same as the reference ion. In measuring the fragments of CH_n^+ ($n = 0$–4), where the initial average kinetic energy of the fragments is less than 0.5 eV [9], the collection efficiency for these fragments is expected to be unity. The mass of these fragments ranges from 12 to 16, and the instrumental effect such as the mass dependent transmission of the quadrupole mass spectrometer can be neglected. This was verified by measuring the relative ionization of Ne and N_2. The transmission of the quadrupole was constant within the experimental errors of the cross-section measurements for these two gases [7,11]. The error in the measurements was estimated to be on the order of $\pm 15\%$ by the square root of the sum of the square of different contributions, which include the uncertainty of the cross-section of the reference gas $\pm 7\%$, the pressure stability $< 1\%$, the count rate fluctuation $\pm 8\%$, the electron current reproducibility $< 5\%$, the collection efficiency of the ion-optics and the mass dependent transmission of the mass spectrometer $< 10\%$.

In the measurement of the subsequent ion–molecule reaction products, high backing pressures of 4 bar were used. In this case the gas density in the molecular beam was estimated to be on the order of $10^{13}/cm^3$, so that extensive ion–molecule reactions occurred. The production of the fragments was measured in a similar manner as mentioned above and was also normalized to the result of CH_4^+ to eliminate the instrumental factors in the measurements.

3. Results and discussions

3.1. Measurements of the cross-section for dissociative ionization

The result for direct ionization of methane is shown in Fig. 2. For comparison, the tabulated data of Adamczyk et al. [12], Orient and Srivastava [4], and Straub et al. [6] are also included. The data for the work of Chatham et al. [13] and Tarnovsky et al. [5] were taken from their published curves. We see
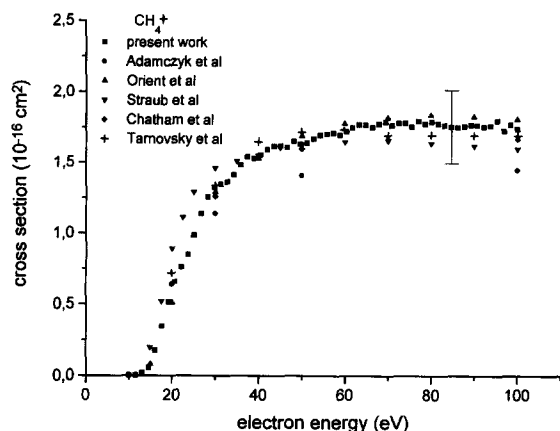
Fig. 2. The cross-section of direct ionization, the previous results are included for comparison.

Fig. 3. The cross-section of the dissociative ionization to CH_3^+, the previous results are included for comparison.

that our results are in overall agreement with all the previous results. However, we like to point out that at lower electron energies, e.g. 25 eV, the very recent results of Straub et al. lie above all the other results including ours. The difference between the results even exceeds the claimed errors. At this low electron energy, the cross-section increases steeply and the ions are produced in a very low translational energy, so that the collection efficiency in different measurement techniques cannot cause the difference in the measurements. The calibration of the electron energy, as well as the width of the electron energy distribution are very important. Another possible reason is that the present work, like that of Orient and Srivastava and that of Tarnovsky et al. was normalized to the reference gas. If the measurement for the reference gas at low electron energy had a higher uncertainty, the difference between these results and Straub et al. will be larger. In order to compare the
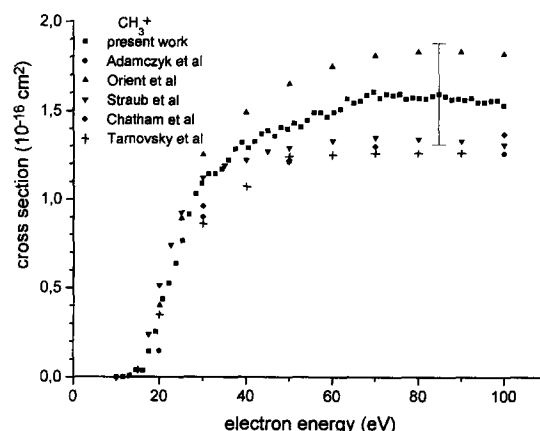
results more quantitatively, we tabulated the results at 100 eV for the different measurements. The stated maximum kinetic energy with unity collection efficiency in the measurements and the error range claimed by the authors are also included in Table 1.

The result for the biggest fragment generated by dissociative ionization, CH_3^+, is shown in Fig. 3. Here the result of Orient and Srivastava are well above the others and the difference is larger than the errors claimed by the different authors (see Table 1). Our result lies in between that of Orient and Srivastava and the others. From Table 1 we see that the fast beam apparatus of Tarnovsky et al. [5] can collect the ions with the initial kinetic energy of less than 2 eV. Furthermore the pulsed extraction system of Orient and Srivastava [4] collects all the ions with less than 5 eV initial energy. Finally the short-path-length time-of-flight (TOF) mass spectrometer of Straub et al. [6] can collect all the ions. Since CH_3^+

Table 1
The cross-section (in 10^{-18} cm^2) of dissociative ionization of methane at the electron energy of 100 eV

CH_4^+	CH_3^+	CH_2^+	CH^+	C^+	Max. kinetic energy of unity collection	Claimed error	Ref.
145	126	21	9.7	3.5			[12]
167	137	23	10	3.3		±15%	[13]
181	182	26	10.9	4.3	5 eV	±15%	[4]
174	130	30	10 [a]		2 eV	±18%	[5] [b]
160	131	31.2	17	6	> 10 eV	±5%	[6]
173	157	26.7	13.2	4.9	3 eV	±15%	present work

[a] The value at 70 eV. [b] The results from the CD_4.

Fig. 4. The cross-section of the dissociative ionization to CH_2^+, the previous results are included for comparison.
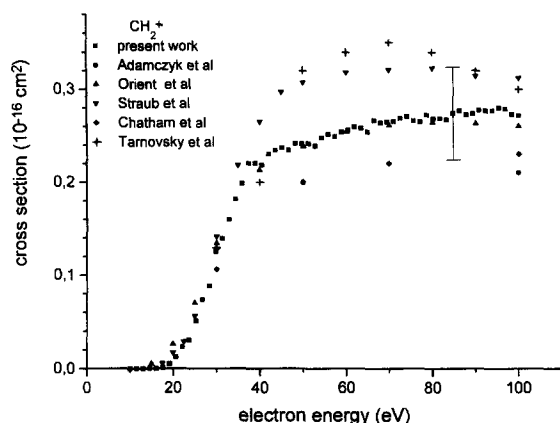

Fig. 6. The cross-section of the dissociative ionization to C^+, the previous results are included for comparison.

is generated at a very small average kinetic energy of less than 0.1 eV, it is of similar mass to the parent ion and has a similar transmission through the quadrupole mass spectrometer. The difference between the results of Orient and Srivastava and the others cannot be explained by the collection efficiency and by the mass and energy dependent transmission of the mass spectrometer.

The result for CH_2^+ is shown in Fig. 4. Here our result agrees very well with that of Orient and Srivastava, but lies below the fast beam result of Tarnovsky et al. and the TOF result of Straub et al. The results for CH^+ and C^+ are shown in Fig. 5 and Fig. 6, respectively. As noted by Straub et al. [6],
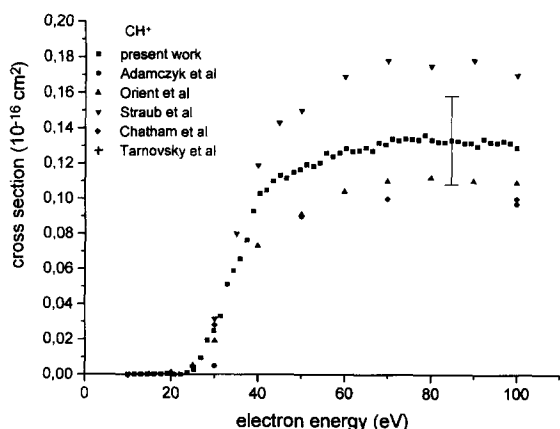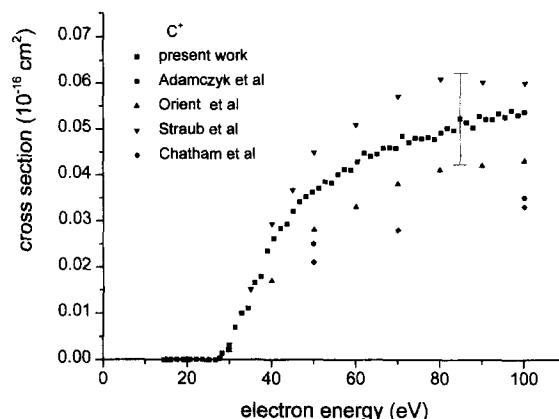
their values are well above the previous measurements, and in fact, their values are also above our measurements, although our results are already above the previous results. In the dissociation of CH_4, the average kinetic energies of CH^+ and C^+ are on the order of 0.2 eV and 0.3 eV [9] respectively, so we believe the collection efficiency in different measurements cannot cause the big experimental difference. The cross-section for the smaller fragments should be further confirmed using different measurement techniques.

Fig. 5. The cross-section of the dissociative ionization to CH^+, the previous results are included for comparison.
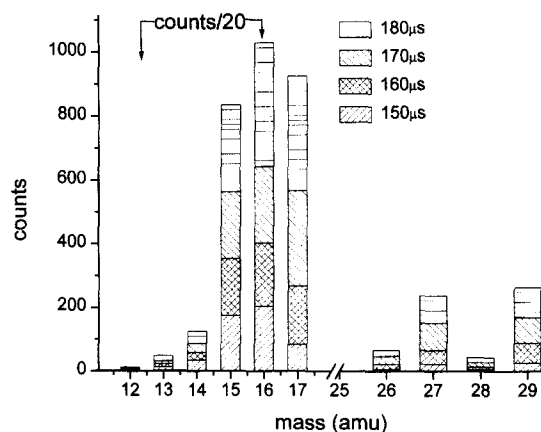

Fig. 7. The mass spectra of the reactant ions and the product ions, the counts of reactant ions are shown in 1/20. The backing pressure is 4 bar, and the electric pulses applied to the nozzle are 150, 160, 170,180 μs in duration, respectively.

3.2. The subsequent ion–molecule reactions

When we apply higher backing pressures and longer nozzle pulses, we also observe the ions with mass $m = 17, 26, 27, 28, 29$. The mass spectra at 40 eV at a backing pressure of 4 bar are shown in Fig. 7. The counts at $m = 17$ also include the contribution from $^{13}CH_4^+$. No counts at even bigger masses were observed. Methane dimers, which can be formed in the supersonic expansion of the molecular beam, were known to undergo intracluster ion–molecule reactions which also give the same fragments as above [14–16]. However, in our work we concluded that the fragments were predominantly produced by gas phase ion–molecule reactions by measuring the appearance potential and by seeding methane in an argon carrier gas. The relative count rates of these products are shown in Fig. 8, which have been normalized to the count rates of CH_4^+ to eliminate the geometry factors. The count rates at $m = 17$ have been subtracted by 1.12% of the counts at $m/e = 16$, which is the natural abundance of ^{13}C relative to that of ^{12}C. Thus we get the pure count rates of $^{12}CH_5^+$. We can see that the count rates of CH_5^+ are the highest among these fragments. $C_2H_5^+$ ($m = 29$) and $C_2H_3^+$ ($m = 27$) have similar count rates. Also $C_2H_4^+$ ($m = 28$) and $C_2H_2^+$ ($m = 26$)

Table 2
Summary of the product branch ratio (in percent) of the reactions between CH_n^+ ($n = 0$–4) and methane at thermal energy and 4.2 eV [17–20]

Reactant ion	kinetic energy (eV)	CH_5^+	$C_2H_2^+$	$C_2H_3^+$	$C_2H_4^+$	$C_2H_5^+$
CH_4^+	thermal	100	0	0	0	0
	4.2	40	0	0	0	0
CH_3^+	thermal	0	0	0	0	100
	4.2	0	0	71	0	29
CH_2^+	thermal	0	0	0	30	70
	4.2	0	22	69	0	0
CH^+	thermal	0	12	83	5	0
	4.2	0	100	0	0	0
C^+	thermal	0	50	50	0	0
	4.2	0	30	25	0	0

have similar count rates. The appearance potential of CH_5^+ lies at 12.8 ± 0.5 eV, which is similar to that of CH_4^+ (12.6 eV). $C_2H_5^+$ ($m = 29$) and $C_2H_3^+$ ($m = 27$) have the same appearance potential, which lies at 14.2 ± 0.5 eV. Similarly, $C_2H_4^+$ ($m = 28$) and $C_2H_2^+$ ($m = 26$) have an appearance potential, which lies at 16.2 ± 1 eV. These appearance energies are very different from those measured in ion–molecule reactions within clusters [16], and verify that the bigger fragments are produced by gas phase ion–molecule reactions.
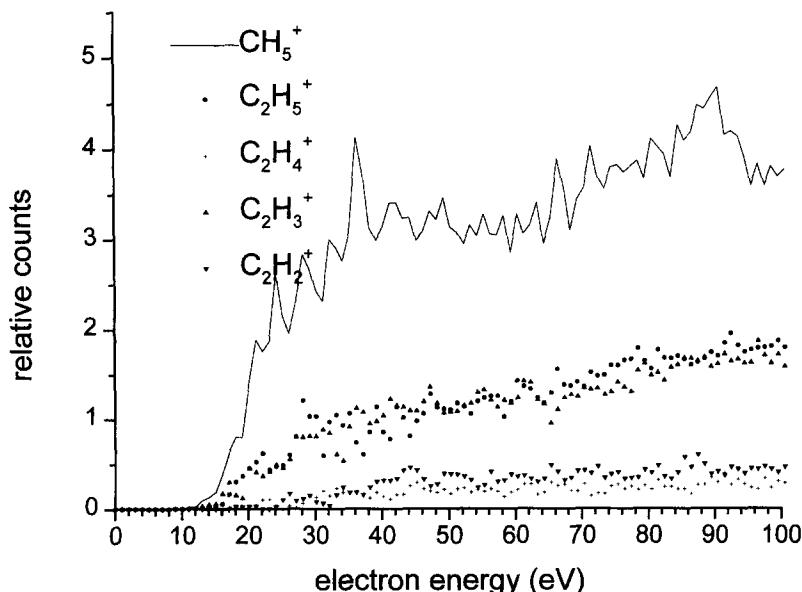

Fig. 8. The relative counts of the product ions at the electron energy from the threshold to 100 eV.
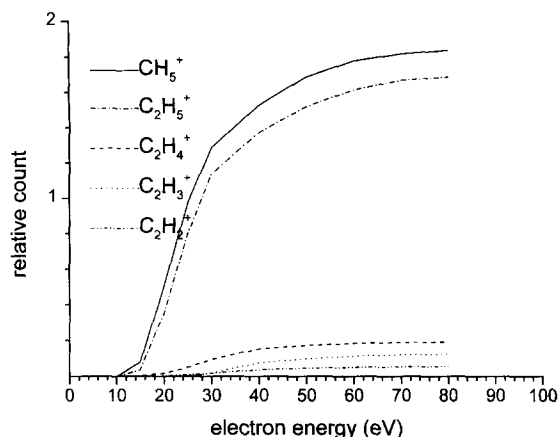
Fig. 9. The calculated result using the ion–molecule reaction product ratios at thermal energy.

The ion–molecule reactions between the ions of CH_n^+ ($n = 0$–4) and methane have been studied since the 1960s due to the importance of the reactions in interstellar chemistry [17–20]. The rate constants, the branching ratios of the products at different collision energies have been well-established [21]. The rate constant of these reactions is of the order of 1.0×10^{-9} cm^3/s. Initially we thought that the reactions in the methane beam is near the thermal collision energy due to the field-free interaction region and the low kinetic energy of CH_n^+ ($n = 0$–4) ions produced in the dissociation. When we used the literature values for the branching ratios of the products at thermal energies, which are summarized in Table 2, and the measured cross-sections for dissociative ionization of methane described above, to calculate the relative products in the methane beam, the results are very different from our measurements. The calculated thermal energy results are shown in Fig. 9, which show a much higher relative intensity of $C_2H_5^+$, but a much lower intensity of $C_2H_3^+$. The intensity of $C_2H_2^+$ is also higher than that of $C_2H_4^+$ in the measurements. The difference between calculation and measurements can be explained if we note that the extraction field accelerates the reactant ions to higher kinetic energies and some reactions occur further down on the path way when the ions are flying to the mass spectrometer. Table 2 also shows that at higher kinetic energies the reactions tend to produce lighter fragments. From this we can qualitatively explain the higher count rates of the lighter

fragments, and the same appearance potential of $C_2H_5^+$ and $C_2H_3^+$.

4. Summary

The cross-sections for the electron impact dissociative ionization of methane have been measured. For direct ionization our results agree well with the previous measurements. For the fragments of CH_3^+, CH_2^+, CH^+, and C^+, our results overlap with the previous measurements where the disagreement between them is bigger than the errors claimed by the different authors. The possible reason for the disagreement between the different measurement techniques has been discussed. At higher backing pressures the subsequent ion–molecule reactions have been observed. The relative production of the product ions were explained qualitatively using the ion–molecule reaction results in literature.

References

[1] C.M. Leung, E. Herbst, W.F. Huebner, Astrophys. J. Suppl. Ser. 56 (1984) 231.
[2] E. Herbst, C.M. Leung, Astrophys. J. Suppl. Ser. 69 (1989) 271.
[3] A.L. Hughes, E. Klein, Phys. Rev. 23 (1924) 450.
[4] O.J. Orient, S.K. Srivastava, J. Phys. B. At. Mol. Phys. B 20 (1986) 3924.
[5] V. Tarnovsky, A. Levin, H. Deutsch, K. Becker, J. Phys. B: At. Mol. Opt. Phys. 29 (1996) 139.
[6] H.C. Straub, D. Lin, B.G. Lindsay, A. Smith, R.F. Stebbings, J. Chem. Phys. 106 (1997) 4430.
[7] D. Rapp, P. Englander-Golden, J. Chem. Phys. 43 (1965) 1464.

[8] J.A. Syage, J. Chem. Phys. 97 (1992) 6085.

[9] I. Ben-Itzhak, K.D. Carnes, S.G. Ginther, D.T. Johnson, P.J. Norris, O.L. Weaver, Phys. Rev. A. 47 (1993) 3748, and references therein.

[10] R. Locht, J.L. Oliver, J. Momigny, Chem. Phys. 43 (1979) 425.

[11] E. Krishnakumar, S.K. Srivastava, J. Phys. B. At. Mol. Opt. Phys. 23 (1990) 1893.

[12] A.J. Adamczyk, H. Boerboom, B.L. Schram, J. Kistemaker, J. Chem. Phys. 44 (1966) 4640.

[13] H. Chatham, D. Hils, R. Robertson, A. Gallagher, J. Chem. Phys. 81 (1984) 1770.

[14] A. Ding, J. Hesslich, Extended Abstracts, ICPEAC 13, Berlin, 1983; 9th Int. Symp. Molecular Beams, Freiburg, 1983.

[15] A.C. Kummel, R.A. Haring, A. Haring, A.E. de Vries, Int. J. Mass Spectro. Ion Proc. 61 (1984) 97.

[16] A. Ding, R.A. Cassidy, J.H. Futrell, L. Cordis, J. Phys. Chem. 91 (1987) 2562.

[17] F.P. Abramson, J.H. Futrell, J. Chem. Phys. 45 (1966) 1925.

[18] R.D. Smith, J.H. Futrell, J. Chem. Phys. 65 (1976) 2574.

[19] N.G. Adams, D. Smith, Chem. Phys. Lett. 47 (1977) 383.

[20] M. Tichy, A.B. Rakshit, D.G. Lister, N.D. Twiddy, Int. J. Mass Spectro. Ion Phys. 29 (1979) 231.

[21] V.G. Anicich, W.T. Huntress, Jr. Astrophys. J. Supp. Ser. 62 (1986) 553, and references therein.